Stress-induced formation of high-density amorphous carbon thin films

J. Schwan,[a] S. Ulrich, T. Theel, H. Roth, and H. Ehrhardt
Universität Kaiserslautern, FB Physik, 67663 Kaiserslautern, Germany

P. Becker
Universität Kaiserslautern, IFOS, 67663 Kaiserslautern, Germany

S. R. P. Silva
University of Surrey, Electronic and Electrical Engineering, Guildford, Surrey GU2 5XH, England

(Received 29 July 1996; accepted for publication 22 August 1997)

Amorphous carbon films with high sp^3 content were deposited by magnetron sputtering and intense argon ion plating. Above a compressive stress of 13 GPa a strong increase of the density of the carbon films is observed. We explain the increase of density by a stress-induced phase transition of sp^2 configured carbon to sp^3 configured carbon. Preferential sputtering of the sp^2 component in the carbon films plays a minor role compared to the $sp^2 \Rightarrow sp^3$ transition at high compressive stress formed during the deposition process. Transmission electron microscopy shows evidence of graphitic regions in the magnetron sputtered/Ar plated amorphous carbon thin films. Differences in the microstructure of the tetrahedral amorphous carbon (ta–C) films deposited by filtered arc and mass selected ion beam; and those films deposited using magnetron sputtering combined with intense ion plating can be used to explain the different electronic and optical properties of both kinds of ta–C films. © *1997 American Institute of Physics.* [S0021-8979(97)09422-X]

INTRODUCTION

Carbon films have been of considerable research interest since Aisenberg and Chabot[1] deposited the first hard, diamondlike amorphous carbon films. Amorphous carbon films with a high fraction of sp^3 hybridized carbons have been deposited by filtered cathodic vacuum arc (FCVA)[2–4] and mass selected ion beams.[5–8] C^+ ions are used to deposit the amorphous carbon films by both techniques. Different mechanisms for the formation of the sp^3 rich phase have been proposed such as the shallow implantation process (subplantation) by Lifshitz *et al.*,[5,6] selective sputtering processes by Reinke and Kuhr[9] (discussed for *c*-BN), and stress-induced phase transition processes by McKenzie *et al.*[3,10] Analytical expressions for the subplantation process describing the formation of stress and the densification have been proposed by Davis[11] and Robertson.[12] The basic idea of the models by Davis and Robertson is that a carbon ion needs at least the displacement energy to penetrate into the carbon film leading to a densification of subsurface layers of the evolving film.[6] But, not all the energy of the energetic carbon ion is used for penetration (displacement processes). Part of the ion energy is used by momentum transfer collisions which results in a thermal spike. Davis[11] and Robertson[12] modified calculations of Windischmann[13] by allowing implanted carbon atoms to relax to the film surface, due to the high localized temperature generated by the impinging C^+ ions in the thermal spike. Yet, questions as to the validity of a thermal spike at ion energies of a few hundred electron volts in a low elemental mass material remains unanswered. Nevertheless, at such impact energies several thousand vibrations are involved for a time period of the order of 10^{-12} s.[14]

Dense and highly tetrahedral amorphous carbon films have also been deposited by the laser ablation technique,[15,16] by dual ion beam technique,[17] and recently by magnetron sputtering together with intense ion plating (MS/IP).[18,19] This MS/IP technique differs from other techniques since the film forming particles are low energy neutral carbon atoms (sputtered from a graphite target), and the necessary energy for densification of the film is transferred by the argon ion plating process.

In this article evidence as to the influence of stress on the deposition of highly tetrahedral amorphous carbon (ta–C) films by MS/IP is discussed using new experimental results. The relaxation or migration of implanted carbon atoms to the film surface at high plating energies is shown not necessarily to be due to a thermal spike [of Seitz and Koehler (Ref. 20)], but more likely to the enhanced mobility of carbon atoms below the surface resulting from the momentum transfer due to the intense ion bombardment. Further, the article shows for the first time evidence for the existence of ordered regions with interplanar spacings corresponding to graphite even when the bulk density of the films are much higher than that of graphite. These regions explain the different electronic properties of the ta–C films prepared by MS/IP compared to ta–C films prepared by FCVA. Further, we show that there is no straightforward relationship between the sp^2 content and the optical and electronic properties of the amorphous carbon films. We show that beside the sp^2 content, the distribution and local bonding of the sp^2 sites must play a significant role in the electronic and optical properties of *a-C* and *a*-C:H.

EXPERIMENTAL DETAILS

Using MS/IP technique a graphite target is sputtered by Ar ions which derive from the plasma torus in front of the target.[18] In our experiment, the neutral sputtered carbon at-

[a]Present address: SAP AG Postfach 1461, D-69185 Walldorf, Germany; author to whom all correspondence should be addressed.

 0021-8979/97/82(12)/6024/7/$10.00

oms are deposited on crystalline silicon substrates and are hit by argon ions originating from the substrate side of the plasma. As a result of the Ar^+ collisions, the carbon atoms at the surface of the film are forced into the film. Amorphous carbon films have been deposited by unbalanced magnetrons using the dc- and rf-mode. In the dc-mode the unbalanced magnetron works at power levels between 20 and 200 W. In this study the magnetron operates in the rf-mode at an Ar pressure of 1.5×10^{-3} mbar, a rf power of 200 W with a rf-frequency of 13.56 MHz. The target to substrate distance is 6 cm for both magnetrons. Using the magnetron working in the rf mode the energy of the plating Ar ions is varied by applying an additional bias to the substrate from 25 (plasma potential) to 150 eV. The experiments for the rf unbalanced magnetron have been carried out at different ratios of Ar ion flux, ϕ_i, to carbon atom flux, ϕ_n, here especially for $\phi_i/\phi_n=3$ and 8. The stress of the deposited films have been measured by the bending beam method using Stoney's equation.

The film density values have been derived from the plasmon energy obtained from electron energy loss spectroscopy (EELS) and by Rutherford backscattering spectroscopy (RBS). Further density measurements of the carbon films prepared with the dc magnetron have been performed by a floating method, where the films were placed in a solution which had a graded density. In addition, the density has also been determined by a weighing method which measured the mass and the volume of the film. It should be noted that EELS is a measure for the electron density.

Electron spin resonance (ESR) measurements have been performed at a microwave frequency of $\sim$9.3 GHz using a microwave power of 25 μW in order to avoid saturation effects. Only for the samples showing a very low spin density was a microwave power of 0.25 mW chosen. The ESR measurements were carried out at room temperature at a modulation amplitude of 0.9 Gauss with a modulation frequency of 100 kHz. The spin densities of the films have been determined by comparison to a standard (DPPH).

Further measurements have been performed using transmission electron microscopy (TEM) at an accelerating voltage of 200 kV.

RESULTS AND DISCUSSION

An unbalanced dc magnetron has been used to deposit *a*-C films at rather low argon plating energies and different flux ratios ϕ_i/ϕ_n (Fig. 1). The carbon film densities of Fig. 1 have been measured by different methods. The difference between the densities as measured by the weighing method and densities determined by EELS (or floating method) can be understood if the microstructure of the carbon film is considered. The weighing method is performed by weighing the mass and measuring the volume from the thickness, and area of the deposited carbon film. Therefore, microvoids may contribute significantly to the volume of the film. The densities of the carbon films as determined by the floating method and EELS measurement remains approximately constant at a value of 2.1 g/cm^3. Both methods do not depend strongly on microvoids in the films as in case of the weighing method.

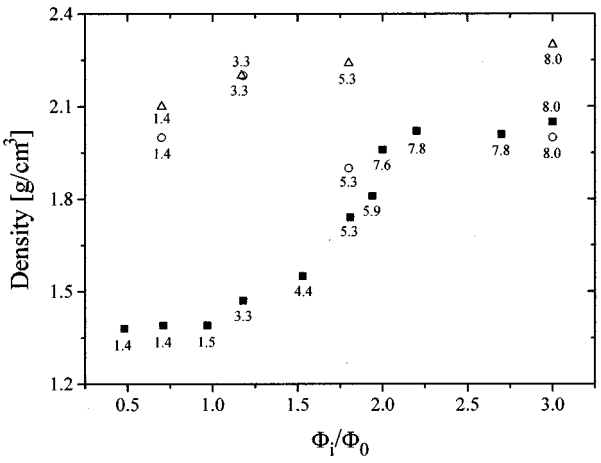

FIG. 1. Density of carbon films deposited by a dc unbalanced magnetron. The Ar plating energy has been varied by changing the dc power (from 200 down to 20 W) and pressure in the deposition chamber (from 3×10^{-2} to 2×10^{-3} mbar). The density of the films has been measured by three different methods, (■) density measured by a weighing method, (○) density measured by a floating method, (△) density derived from the EELS plasmon energy. The small numbers at the symbols represent the energy of the plating Ar.

Thus, the density as determined by EELS is a measure of the density of the local bonding structure (we refer to the density measured by the EELS method as microdensity), whereas, the density as determined by the weighing method is a macro(scopic) density. This means that the density results can be explained by a carbon structure with a density close to graphite (around 2.2 g/cm^3) but containing microvoids. From Fig. 1, one possible conclusion that can be drawn is that most microvoids are essentially compressed in a carbon matrix deposited at plating energies >7 eV and flux ratios >2. These findings are in agreement with theoretical predictions of Muller.[21]

In this article we describe experiments pertaining to the deposition of amorphous carbon films using an unbalanced magnetron working in the rf mode and with rather high ϕ_i/ϕ_n ratios. EELS measurements have been performed to determine the microdensity of the carbon films for flux ratios of 3, 5, 8, and 10 and have been confirmed by RBS. The energy dependence of the microdensity for the flux ratios of 5 and 10 was published elsewhere.[18] The results show that for flux ratios of 5, 8, and 10 a maximum in the microdensity is found. For a flux ratio of three no significant densification of the carbon films can be observed as a function of the ion plating energy. The microdensity of these films remain constant at a value of 2.1 g/cm^3 (Fig. 2). For a ϕ_i/ϕ_n ratio of 10, a maximum density of 3.1 g/cm^3 and sp^3 content of 87% has been recorded for an Ar energy of 90 eV (*K*-edge EELS spectra are shown in Fig. 3). For a ϕ_i/ϕ_n ratio of 8 the peak values of density amount to 2.6 g/cm^3 at an Ar energy of 98 eV. For a ϕ_i/ϕ_n ratio of 5 the peak values of density and sp^3 amount to 2.6 g/cm^3 and 60% at an Ar energy of 105 eV. The densities calculated by EELS show a similar behavior to the densities determined by RBS [they also reveal maxima in the density at ion energies of 90 eV (for ϕ_i/ϕ_n ratio of 10), 98 eV (ϕ_i/ϕ_n ratio of 8) and 105 eV (ϕ_i/ϕ_n ratio of 5)].

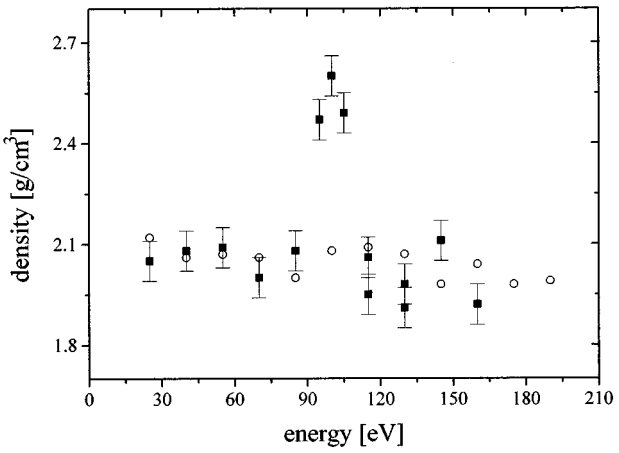

FIG. 2. Microdensity derived from transmission EELS plasmon energy of a-C films deposited by unbalanced rf magnetron for flux ratios $\Phi_i/\Phi_n=3$ [○] and 8 [■].

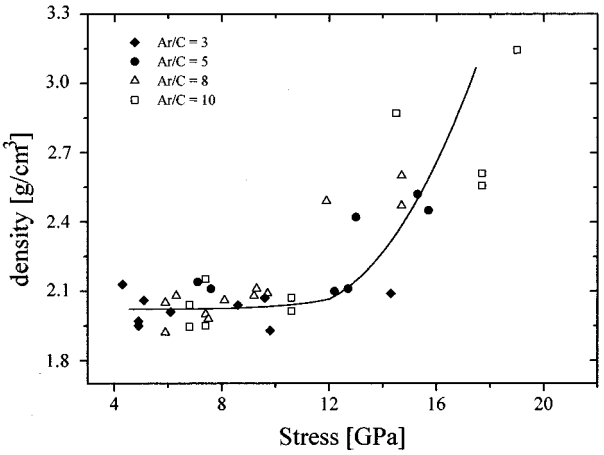

FIG. 4. Density vs stress for flux ratios $\Phi_i/\Phi_n=3$ (♦), 5 (●), 8 (△), and 10 (□). A stress threshold at 13 GPa is observed.

The density calculated from RBS data is 20% higher than the density calculated from EELS data. This is not surprising because the depth resolution of RBS at a depth of 1000 Å is about 200 Å due to multiple scattering of the ions (electronic stopping). Thus, it is expected that densities calculated from RBS-data have higher density values compared to densities calculated from EELS-data.

For completeness we present the microdensity dependence on stress for films deposited at flux ratios ϕ_i/ϕ_n of 3, 5, 8, and 10 (Fig. 4) although some of the data have already been published.[18] Since only the microdensity is measured, it is still possible that the macrodensity too increases over the entire range presented. But, it should be noted from the results shown in Fig. 1 that in the case of the dc magnetron, for plating energies above 7 eV, and flux ratios of 2, the microdensity and density (measured by other methods) converge to similar values such that the density shown (derived from EELS) is a good measure for the real density of the carbon films. In Fig. 4 we see a marked increase in density above a compressive stress of 13 GPa, which indicates the existence of a stress threshold for the formation of a highly dense carbon structure such as those found with high sp^3 contents. Figure 4 also indicates that for the formation of dense amorphous carbon films by MS/IP high flux ratios are required. The stress threshold of 13 GPa can be compared to the pressure values found by Erskine *et al.*,[22] Yagi *et al.*,[23] Takano *et al.*,[24] and Endo *et al.*[25] for transitions from graphite to a denser form of carbon. Below the stress transition value, the films have a density close to that of graphite and the other physical properties such as optical band gap are graphitelike.[18] These can be compared to values normally found for magnetron sputtered carbon films.[26] The carbon films with the highest density (3.1 g/cm^3) has the highest sp^3 content (87%) and an optical gap of 1 eV. This very low value for the optical gap is not consistent with that for ta–C films (up to 2 eV) with comparable sp^3 contents prepared by the filtered cathodic vacuum arc,[2] but, shows similarities to data of Ishikawa *et al.*[27] for C^- ion deposition of highly ta–C films. In Fig. 5 we present experimental data indicating that no inconsistency exists between the low optical gap of 1 eV and high sp^3 content of 87%, by showing that a relationship does not exist between the sp^2 content and the optical band gap in a–C and a–C:H films. The correlation between

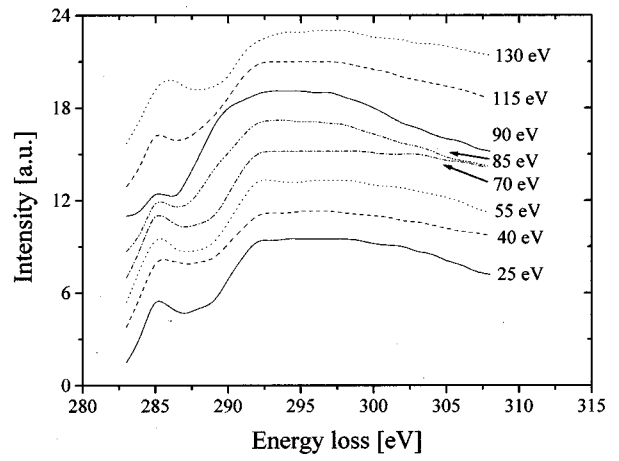

FIG. 3. K-edge EELS spectra for $\Phi_i/\Phi_n=10$ for different ion energies.

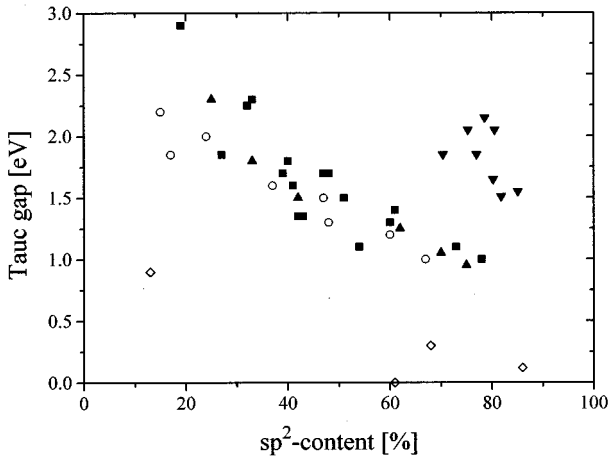

FIG. 5. Optical gap vs sp^2 content Chowahlla *et al.* (○) (Ref. 28), Kleber *et al.* (Ref. 29), Tamor *et al.* (Ref. 30) (■), Weiler *et al.* (▲) (Ref. 31), Batori *et al.* (▼) (Ref. 32), and this work (◇).

the sp^2 content and optical gap is not straight forward. Beside the sp^2 content the distribution and local bonding of the sp^2 bonds also plays a significant role in the electronic properties of the amorphous (hydrogenated) carbon films.

The stress and the microdensity are also not linearly coupled to each other in the case of indirect subplantation; which is different for the case of direct C^+ implantation.[12] The inefficiency for the densification process and the creation of high stresses due to knock on effects will now be discussed in more detail. In the case of knock on processes, the formation of an interstitial in a subsurface layer is accompanied by the generation of a vacancy at the surface due to the argon bombardment. The interstitial leads to an increase in densification and stress in the subsurface while the vacancy at the surface leads to a reduction in density at the surface. The results presented show that the microdensity remains constant at ≈ 2.1 g/cm^3 while the compressive stress in the films remains below 13 GPa. Despite the stress increasing with increasing argon ion energy (up to 100 eV), the nonvariance of the density indicates that the implanted (knocked on) carbon is not trapped in the carbon film as a density increasing interstitial. Due to the low energy involved in the knock on process, the interstitial is created near the vacancy close to the surface. This vacancy does not exist in the direct subplantation process. In the indirect subplantation process the implanted carbon can more easily migrate to the surface due to the close proximity of the missing carbon at the surface. This relaxation process leads to the comparatively higher inefficiency of densification compared to the direct subplantation process. Yet, the migration of the subsurface interstitial to the surface does not necessarily mean that the stress in the film is relieved. The stress is likely to remain in the surrounding matrix although the cause of the stress has now been removed. Thus, high stresses can be created with no apparent densification. Up to 13 GPa, relaxation processes like the one described above dominate. As the stress exceeds the threshold of 13 GPa the $sp^2 \rightarrow sp^3$ transformation takes place.

For all Φ_i/Φ_n ratios, the stress versus ion energy curves show distinct maxima depending on both, the ion energy and ϕ_i/ϕ_n values (Fig. 6). Based on calculations of Sigmund,[33] Windischmann,[13] Seitz and Koehler,[20] and Davis[11] found that the stress, σ, varies as a function of the ion energy as follows:

$$\sigma \propto \frac{E^{1/2}}{R\Phi_n/\Phi_i + k \times E^{5/3}}, \tag{1}$$

where Φ_i equals the ion flux, Φ_n is the total flux per unit area with which atoms contribute to the growing film, R and k are constants which depend on the density and the activation energy for the relaxation process. This analytical expression was derived for films deposited at low ion plating energies (0–150 eV).

It has already been shown that the plating Ar^+ does not densify the carbon film as efficiently as an implanted C^+ ion.[18] This implies that the excess energy in the case of argon ion plating must be higher than in the case of direct carbon ion implantation, because a stronger migration of implanted carbon to the surface takes place. This also indicates that the

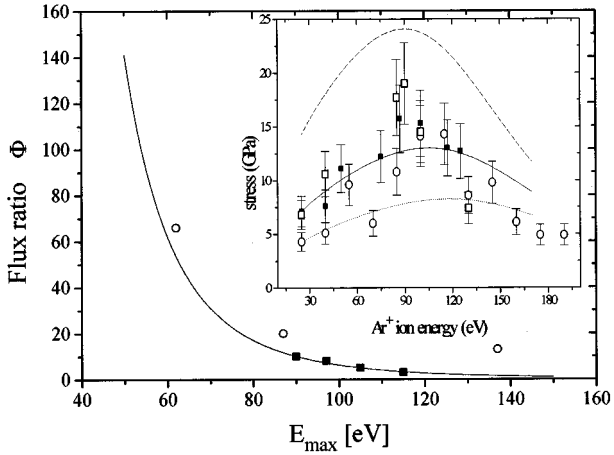

FIG. 6. Energy position $E_{\max}$ of the stress maximum vs flux ratio Φ_i/Φ_n for carbon films deposited by MS/IP (■). The open symbols present data points for c-BN films deposited by the same technique (Refs. 30 and 31). The function through the points (full line) is given by $\Phi_i/\Phi_n(E) = 3.5\ (\mathrm{eV})^{4.5}/8 \times E^{4.5} \times 7.0 \times 10^{-11}$. The insert shows the stress behavior for films deposited at flux ratios of $\Phi_i/\Phi_n = 3$ (○), 5 (■), and 10 (□) together with the calculated stress behavior using the constants R, k, and x in Eq. (1).

deposition process above the maximum should not be dominated by $E^{-5/3}$, but, by an energy dependence E^{-x} where $x > 5/3$ for the films deposited by magnetron sputtering and intense ion plating.

Considering $d\sigma/dE|_{E_{\max}} = 0$ at the energy position $E_{\max}$ of the stress maximum we calculate (not fit) from two experimental data points of $\Phi_i/\Phi_n = 5$ ($E_{\max}$ amounts to 105 eV), and for $\Phi_i/\Phi_n = 10$ ($E_{\max}$ amounts 90 eV) a value for $x = \ln(10/5)/\ln(105/90) = 4.5$. This means that the relaxation in the case of the indirect subplantation process is not due to a thermal spike as discussed by Seitz and Koehler,[20] but another relaxation/migration or diffusion process due to the enhanced mobility of the carbon atoms resulting from the intense ion bombardment. It is emphasized that the value $x = 4.5$ is an empirical value and is not derived for a special relaxation or migration process. Taking only one experimental data point at a stress value of 13 GPa for $\Phi_i/\Phi_n = 5$ at $E_{\mathrm{ion}} = 105$ eV the constants R and k can be calculated using Eq. (1) and $d\sigma/dE|_{E_{\max}} = 0$. The simple flux and energy dependence (found by two data points) based on the model of Davis[11] and Robertson[12] describes the stress variation for the different flux ratios of 3, 5, 8, and 10 (in dependence of the energies) well. Further, from the calculated constants it is possible to determine the flux ratio as a function of the ion energy, where the density and stress reveal a maximum value:

$$\Phi_i/\Phi_n(E) = \frac{3.5\ (\mathrm{eV})^{4.5}}{8 \times E^{4.5} \times 7.0 \times 10^{-11}}. \tag{2}$$

This curve is plotted in Fig. 7 together with data for MS/IP ta–C films (■). Further, values for c-BN (O) as found by Ulrich *et al.*[34,35] are introduced into Fig. 7. It shows that for c-BN and ta–C films deposited by the same ion plating

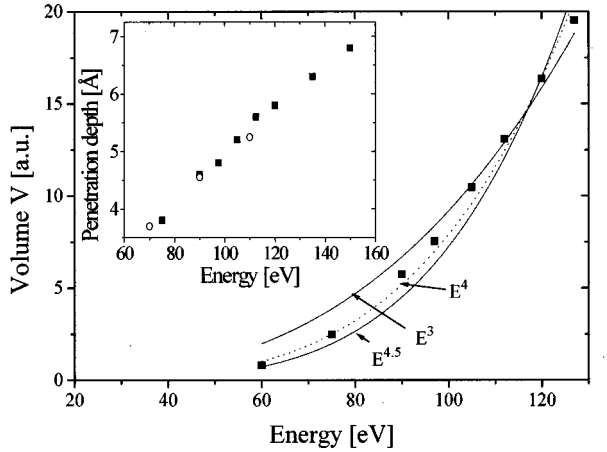

FIG. 7. Volume V, where the argon ion looses all its energy in dependence of Ar ion energy with Ar ion energies varying between 80 and 130 eV. The volume V' is calculated using the TRIM code of Biersack *et al.* (Ref. 36) and a displacement energy of 35 eV. The insert shows the penetration depth R of the argon ions by TRIM calculations (■) and molecular dynamic calculations (○) (Ref. 37) in dependence of the ion energy.

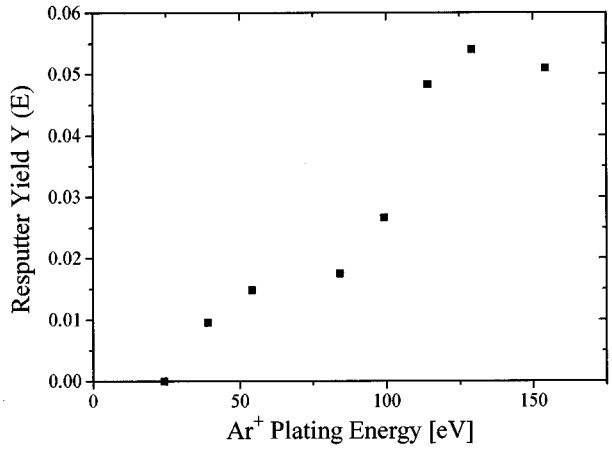

FIG. 8. Resputter yield of carbon vs argon ion plating energy. This figure also shows that the preferential etching only plays a minor role for the creation of sp^3.

technique comparable results are obtained. In both cases the densification leads to higher concentrations of sp^3 bonds.

A possible explanation for the $E^{4.5}$ dependence could be as follows: When an argon ion hits the surface, it transfers its kinetic energy to the carbon atoms close to the surface. If we assume that only carbon atoms, which were knocked by the argon, can move to the surface (radiation enhanced diffusion[5,6]), it is possible to estimate the relaxation of the carbon atoms to the surface as a function of argon ion energy. We assume that only those carbon atoms contained within the volume V, the volume in which an energetic Ar ion loses all its energy (thus having no further energy for displacement processes), contribute to the migration process. The volume V may be estimated using a TRIM cascade algorithm,[36] although strictly speaking the ion energies are too low to give accurate results. TRIM reveals the average lateral straggle ΔR of the argon atoms as well as the penetration range R of the argon ions. Thus, the volume V can be estimated as $V=4/3\pi R(\Delta R)^2$. An ellipsoid volume has been used because the dissipation distribution of the impact energy is symmetric in rotation (thus $V\propto\Delta R^2$) having a Gaussian shape at a penetration depth R. The dependence of V up to an argon ion plating energy of 130 eV is presented in Fig. 5 showing a power law dependence of V vs E^4. This is close to the value of 4.5 found from our experimental results. Still those TRIM calculations have to be confirmed by molecular dynamic calculations. Nevertheless, this would mean that the relaxation is given by the knock on dynamics and energy transfers of the argon ion to the surrounding carbon atoms. Thus, the carbon atoms gain enough energy for a ''radiation enhanced diffusion'' as predicted by Lifshitz.[6]

From the deposition rate, the density and the ion flux, the resputter yield of carbon can be calculated from the experimental data (assuming for an Ar ion plating energy of 25 eV no carbon is resputtered and so the neutral carbon flux Φ_n is given). At the different ion energies the film forming carbon flux is determined by $\Phi_{\mathrm{Dep}}=\rho N_A d/m_C$ (m_C=carbon mass in amu, N_A=Avogadro constant, d=deposition rate, and ρ=density). The sputtered carbon is then given by $\Phi_s=\Phi_n-\Phi_{\mathrm{Dep}}$ and the resputter yield of carbon is $Y(E)=(\Phi_n-\Phi_{\mathrm{Dep}})/\Phi_i$. The experimental data are shown in Fig. 8 for a flux ratio Φ_i/Φ_n of 10. It appears from Fig. 8 that the sp^2 carbon is preferentially sputtered for the films deposited with high Ar^+ plating energies. If preferential sputtering was the dominant deposition mechanism for the formation of sp^3 bonds all films deposited at high energies should have high sp^3 contents and consequently high compressive stresses. But, it is clearly seen that the sp^3 content and stress both peak at an energy window in the mid-energy region (about 100 eV) depending on the flux for MS/IP films. Therefore, preferential sputtering in the case of intense ion plating is not responsible for the formation of the sp^3 rich films. This leads to the conclusion that in our case, preferential sputtering has only a weak influence on the deposition mechanism.

To get more information about the microstructure of the a-C films Raman and ESR measurements have been performed. The spin density dependence on Ar ion plating energy for $\Phi_i/\Phi_n=3$ is shown in Fig. 9. For a plating energy

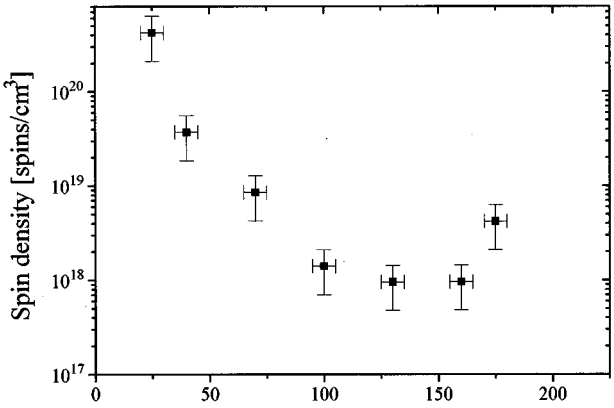

FIG. 9. Spin density vs Argon plating energy for a-C films deposited with the unbalanced rf magnetron at a flux ratio of 3. Further, only for a flux ratio of 5 the spin density could be measured (Ref. 18) because for the films deposited at higher flux ratios the ESR signal was too low.

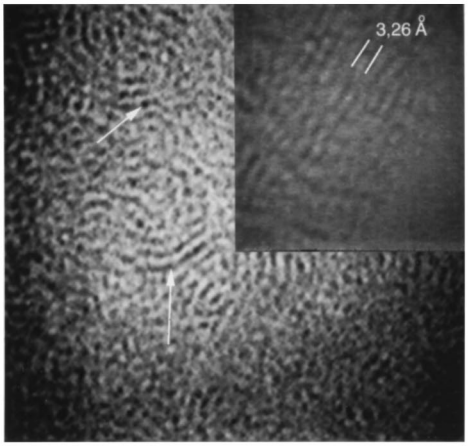

(a)

(b)

FIG. 10. TEM images for a carbon film deposited at a flux ratio $\Phi_i/\Phi_n = 10$ at an energy of 90 eV. The insert shows more clearly the observed stacked parallel fringes having spacings of 3.26 Å. Those fringes cannot be observed in ta–C prepared by the FCVA as shown by Gilkes *et al.* (Ref. 41). The bottom image shows a diffraction pattern of the Ar plated carbon film. The bright arcs show that ordered graphitic regions in the carbon film exist.

of 25 eV the carbon film has a typical defect density of 5×10^{20} spins/cm^3. With increasing plating energy, there is a sharp drop in defect density down to 10^{18} spins/cm^3. The Raman spectra of these films as well as for the amorphous carbon films deposited at higher flux ratios are similar to Raman spectra of highly disordered graphitic structures.[38] This is surprising for carbon films containing more than 60% sp^3, but it should be noted that the Raman sensivity of diamond is 50× less than that for graphite.[39] In order to obtain more information on the microstructure of these films a TEM analysis was performed.

Selected area diffraction was performed using the smallest available aperture. This gave an illuminated region of about 100 nm in diameter. TEM images of carbon films deposited at $\Phi_i/\Phi_n = 10$ and 90 eV Ar^+ plating energy (sp^3 content 87%, density 3.1 g/cm^3) are shown in Fig. 10. The insert in Fig. 10(a) shows a region of the deposited film at higher magnification. The image is taken at the Scherzer defocus condition. At the higher magnification, stacks of parallel fringes can be seen having spacings close to 3.26 Å. This corresponds to the 002 lattice spacing in graphite. Figure 10(b) exhibits the diffraction pattern of the area. Two bright spots can be seen corresponding to the diffraction pattern expected from (002) oriented graphite. This agrees with measurements of McCulloch *et al.*[40] No spots can be observed at the (004) position. The preferentially aligned (002) planes of graphite alludes to the models recently proposed for *a*-C films by McCulloch *et al.*[40] and McKenzie.[3] Although TEM showed that most of the carbon film is amorphous such regions in the carbon films may be responsible for the low optical gap and observed Raman scattering.[38] The rather broad *G*-line width of the Raman data may be due to the high compressive stress in the films.[38] These findings may also explain the ESR results presented. At low plating energy and at low flux ratios, 10^{20} defects/cm^3 have been measured. With increasing plating energy and flux ratio, the π defect centers combine to form saturated π bonds which are not observed as paramagnetic centers by ESR.

SUMMARY

From the measurements presented it can be concluded that the dominant densification process in films deposited by magnetron sputtering and ion plating is a stress induced transformation process from sp^2 carbon to sp^3. The creation of high stress in the films is explained by recoil implantation and relaxation processes due to the intense Ar^+ bombardment during film deposition. Preferential sputtering has only a minor influence on the creation of sp^3 sites. Further, it is shown empirically that the relaxation process is unlikely to be due to a thermal spike. From the measurements presented it can be concluded that ion bombardment creates an enhanced mobility of carbon atoms, below, but close to the surface which leads to a migration of (entrapped recoil) carbon atoms to the surface of the film. The presented results indicate that a more general model is needed to explain the stress (or density) behavior of carbon films with energy. Such a model must take the different diffusion and migration processes into account (e.g., surface diffusion, radiation enhanced diffusion, and volume diffusion).

Even for films with a high sp^3 content, deposited at intense ion flux ratios and Ar ion energies of 90 eV, there is evidence that graphitic regions exist. We propose that in certain localized regions the stress is not sufficiently high to transform graphitic regions to sp^3 bonds. If the stress exceeds a certain threshold, (about 13 GPa) sp^3 rich regions are formed. This means that for the films analyzed in this study, graphitic regions may be the precursor needed for the formation of sp^3 rich films under high compressive stress.

The presented results in this article are evidence that the sp^2 content alone does not control the electronic properties of amorphous (hydrogenated) carbon films. It has to be considered that the local bonding structure of sp^2 carbon (e.g., aromatic, conjugated or olefinic) also plays (beside the sp^2 content itself) a significant role in the electronic properties of the films.

ACKNOWLEDGMENTS

This work was sponsored by the DFG Project No. Eh23/29-1. Most valuable help of Professor Schmoranzer for EELS measurements and of Professor Oechsner for TEM

measurements is gratefully acknowledged. The work of G. Kunz concerning the density measurements at the dc magnetron is gratefully acknowledged.

[1] S. Aisenberg and R. Chabot, J. Appl. Phys. **42**, 2953 (1971).
[2] P. J. Fallon, V. S. Veerasamy, C. A. Davis, J. Robertson, G. A. J. Amaratunga, W. I. Milne, and J. Koskinen, Phys. Rev. B **48**, 4777 (1993).
[3] D. R. McKenzie, D. Muller, and B. A. Pailthorpe, Phys. Rev. Lett. **67**, 773 (1991).
[4] S. R. P. Silva, S. Xu, B. K. Tay, H. S. Tan, and W. I. Milne, Appl. Phys. Lett. **69**, 491 (1996).
[5] Y. Lifshitz, S. R. Kasi, and J. W. Rabalais, Phys. Rev. Lett. **62**, 1290 (1989).
[6] Y. Lifshitz, S. R. Kasi, J. W. Rabalais, and W. Eckstein, Phys. Rev. B **41**, 16 468 (1990).
[7] Y. Lifshitz, G. Lempert, and E. Grossman, Phys. Rev. Lett. **72**, 2753 (1997).
[8] H. Hofsaess and C. Ronning, ASM Conference Proceedings of the International Conference on Beam Processing of Advanced Materials, 1996, p. 29–56.
[9] S. Reinke and S. Kuhr, Diamond Relat. Mater. **3**, 341 (1994).
[10] D. R. McKenzie, D. C. Green, P. D. Swift, D. J. H. Cockayne, P. J. Martin, R. P. Netterfield, and W. G. Sainty, Thin Solid Films **193/194**, 418 (1990); D. R. McKenzie *et al.* Thin Solid Films **206**, 198 (1991).
[11] C. A. Davis, Thin Solid Films **226**, 30 (1993).
[12] J. Robertson, Diamond Relat. Mater. **2**, 984 (1993); *ibid.* **3**, 361 (1994).
[13] H. Windischmann, J. Appl. Phys. **62**, 1800 (1987).
[14] H. Ehrhardt, Adv. Sci. Technol. **6**, 191 (1995).
[15] J. J. Cuomo, J. P. Doyle, J. Bruley, and J. C. Liu, Appl. Phys. Lett. **58**, 466 (1991).
[16] J. J. Cuomo, D. L. Pappas, J. Bruley, J. P. Doyle, and K. L. Saenger, J. Appl. Phys. **70**, 1706 (1991).
[17] B. André, F. Rossi, A. van Veen, P. E. Mijnarends, H. Schut, and M. P. Delplancke, Thin Solid Films **241**, 171 (1994).
[18] J. Schwan, S. Ulrich, H. Roth, H. Ehrhardt, S. R. P. Silva, J. Robertson, R. Samlenski, and R. Brenn, J. Appl. Phys. **79**, 1416 (1996).
[19] S. C. Cheon, D. C. Ingram, and H. H. Richardson, J. Vac. Sci. Technol. A **13**, 2856 (1995).
[20] F. Seitz and J. S. Koehler, Solid State Phys. **3**, 305 (1956).
[21] K. H. Müller, Appl. Phys. A: Solids Surf. **40**, 209 (1986); J. Appl. Phys. **59**, 2803 (1986).
[22] D. J. Erskine and W. J. Nellis, J. Appl. Phys. **71**, 4882 (1992).
[23] T. Yagi, W. Utsumi, M. Yamataka, T. Kigegawa, and O. Shimomura, Phys. Rev. B **46**, 6031 (1992).
[24] K. J. Takano, H. Harashima, and M. Wakatsuki, Jpn. J. Appl. Phys., Part 2 **30**, L860 (1991).
[25] S. Endo, N. Idani, R. Oshima, K. J. Takano, and M. Wakatsuki, Phys. Rev. B **49**, 22 (1994).
[26] S. M. Rossnagel, M. A. Russak, and J. J. Cuomo, J. Vac. Sci. Technol. A **5**, 2150 (1987).
[27] J. Ishikawa, Y. Takeiri, K. Ogawa, and T. Takagi, J. Appl. Phys. **61**, 2509 (1987).
[28] M. Chowahlla, J. Robertson, C. Chen, R. Silva, C. Davis, and G. Amaratunga, J. Appl. Phys. (to be published).
[29] R. Kleber, K. Jung, H. Ehrhardt, J. Muhling, K. Breuer, H. Metz, and F. Engelke, Thin Solid Films **205**, 274 (1991).
[30] M. Tamor and W. Vassel, J. Appl. Phys. **76**, 3823 (1994).
[31] M. Weiler, S. Sattel, T. Giessen, K. Jung, H. Ehrhardt, V. Veerasamy, and J. Robertson, Phys. Rev. B **53**, 1594 (1996).
[32] V. Batori, J. Schwan, S. Ulrich, and H. Ehrhardt, Thin Solid Films submitted.
[33] P. Sigmund, in *Sputtering by Particle Bombardment*, edited by R. Behrisch (Springer, Berlin, 1981), Vol. 1, p. 49.
[34] S. Ulrich, J. Scherer, J. Schwan, I. Barzen, K. Jung, and H. Ehrhardt, Diamond Relat. Mater. **4**, 288 (1995); *ibid.* **5**, 548 (1996).
[35] S. Ulrich, J. Scherer, J. Schwan, I. Barzen, M. Scheib, and H. Ehrhardt, Appl. Phys. Lett. **68**, 909 (1996).
[36] J. Biersack and L. Haggermarck, Nucl. Instrum. Methods **174**, 257 (1980).
[37] P. Deak (personal communication).
[38] J. Schwan, S. Ulrich, V. Batori, H. Ehrhardt, and S. R. P. Silva, J. Appl. Phys. **80**, 440 (1996).
[39] N. Wada, P. Gaczi, and S. Solin, J. Non-Cryst. Solids **35&36**, 543 (1980).
[40] D. G. McCulloch, D. R. McKenzie, and S. Prawer, Philos. Mag. A **72**, 1031 (1995).
[41] K. W. R. Gilkes, P. H. Gaskell, and J. Yuan, J. Non-Cryst. Solids **164–166**, 1107 (1993).